

Radial Dependence of the Pseudodipolar Interaction in White Tin†

S. N. SHARMA AND D. LLEWELYN WILLIAMS

Physics Department, University of British Columbia, Vancouver 8, British Columbia, Canada

AND

HARLAN E. SCHONE

Physics Department, College of William and Mary, Williamsburg, Virginia 23185

(Received 5 May 1969)

The orientation dependence of the nuclear-magnetic-resonance linewidth in a single crystal of isotopically pure Sn¹¹⁹ has been interpreted in terms of the radial dependence of the pseudodipolar interaction. Lorentzian lines have been observed which are consistent with the existence of exchange narrowing and which, together with supplementary measurements of the second moment of the Sn¹¹⁹ resonance in tin of natural isotopic abundance, lead to an estimate of 11 ± 1 kHz for the strength of the scalar exchange interaction.

INTRODUCTION

THE study of the anisotropic properties of the nuclear magnetic resonance in single crystals of metals enables an accurate direct measurement of quantities not readily obtainable from an analysis of data from powdered specimens. To date, studies have been made of the second moments of the resonance line in aluminum,¹ the Knight-shift parameters in tin,^{2,3} cadmium,^{3,4} thallium,⁵ mercury,⁶ gallium,⁷ and magnesium,⁸ and the quadrupole interactions in magnesium⁸ and gallium.⁹ Relaxation-time studies have been made in tin¹⁰ and in copper and aluminum,¹¹ oscillations in the Knight shift with magnetic field have been studied in tin,¹² and the existence of diamagnetic domains has been established in silver.¹³ The present work is concerned with an analysis of the orientation dependence of the resonance line parameters in an isotopically pure single crystal of Sn¹¹⁹, together with some additional measurements upon a specimen of natural isotopic abundance.

† Research supported by the National Research Council of Canada through Grant No. A 1873.

¹ P. L. Sagalyn and J. A. Hofmann, *Phys. Rev.* **127**, 68 (1962).

² E. P. Jones and D. L. Williams, *Can. J. Phys.* **42**, 1499 (1964).

³ S. N. Sharma, Ph.D. thesis, University of British Columbia 1967 (unpublished).

⁴ H. E. Schone, *Phys. Rev. Letters* **13**, 12 (1964).

⁵ J. J. Schratte and D. L. Williams, *Phys. Letters* **26A**, 79 (1967).

⁶ R. W. Weinert and R. T. Schumacher, *Phys. Rev.* **172**, 711 (1968).

⁷ M. Valic, S. N. Sharma, and D. L. Williams, *Phys. Letters* **26A**, 528 (1968).

⁸ P. Dougan, S. N. Sharma, and D. L. Williams, *Can. J. Phys.* **47**, 1047 (1969).

⁹ M. Valic and D. L. Williams, *J. Phys. Chem. Solids* **30**, 2337 (1969).

¹⁰ L. A. McLachlan and D. L. Williams, *Magnetic Resonance and Relaxation* (North-Holland Publishing Co., Amsterdam, 1967), p. 462; L. A. McLachlan, *Can. J. Phys.* **46**, 871 (1968).

¹¹ A. D. Gara, Ph.D. thesis, Washington University, St. Louis, 1965 (unpublished).

¹² J. M. Reynolds, R. G. Goodrich, and S. A. Khan, *Phys. Rev. Letters*, **6**, 609 (1966); S. A. Khan, J. M. Reynolds, and R. G. Goodrich, *Phys. Rev.* **163**, 579 (1967).

¹³ J. H. Condon and R. E. Walstedt, *Phys. Rev. Letters* **21**, 612 (1968).

THEORY

As is well known,¹⁴ the nuclear-magnetic-resonance line-shape parameters are determined by the interaction between the nuclei in the specimen. These comprise not only the direct dipolar interaction, but also the indirect interaction which arises from the coupling of nuclei to the electrons through the hyperfine interaction. The latter is separable into two contributions of differing symmetry whose relative strength depends upon the electron wave functions, namely, the scalar-indirect-exchange interaction of Ruderman and Kittel,¹⁵ which has the form $J_{ij} \mathbf{I}_i \cdot \mathbf{I}_j$, where J_{ij} is the scalar-exchange-constant coupling the nuclear spins \mathbf{I}_i and \mathbf{I}_j , and the pseudodipolar interaction postulated by Bloembergen and Rowland,¹⁶ which has the form $B_{ij}(1 - 3 \cos^2 \theta_{ij}) \times \mathbf{I}_i \cdot \mathbf{I}_j$, where B_{ij} is the pseudodipolar coupling constant and θ_{ij} is the angle between the direction of the applied magnetic field and r_{ij} , the vector joining the two nuclear sites.

The general expression for the second moment of the resonance line from an isotope of abundance f_1 in a specimen containing a second isotope having the same nuclear spin and an abundance f_2 is¹⁶

$$\begin{aligned} \langle \Delta \omega^2 \rangle = & \frac{3}{4} I(I+1) \hbar^{-2} [f_1 \sum (B_{ij} + \hbar^2 \gamma_1^2 r_{ij}^{-3})^2 \\ & + (4/9) f_2 \sum (B_{ij} + \hbar^2 \gamma_1 \gamma_2 r_{ij}^{-3})^2] (3 \cos^2 \theta_{ij} - 1)^2 \\ & + \frac{1}{3} I(I+1) f_2 \sum J_{ij}^2 - \frac{2}{3} I(I+1) \hbar^{-1} f_2 \sum J_{ij} \\ & \times (B_{ij} + \hbar^2 \gamma_1 \gamma_2 r_{ij}^{-3}) (3 \cos^2 \theta_{ij} - 1). \quad (1) \end{aligned}$$

The summation is taken over all nuclear sites, and γ_1 and γ_2 are the gyromagnetic ratios of the two different isotopes.

For the special case of a specimen containing only one isotope with a nuclear spin the expression reduces to

$$\langle \Delta \omega^2 \rangle = \frac{3}{4} I(I+1) \hbar^{-2} f \sum (B_{ij} + \gamma^2 \hbar^2 r_{ij}^{-3})^2 \times (3 \cos^2 \theta_{ij} - 1)^2. \quad (2)$$

¹⁴ J. H. VanVleck, *Phys. Rev.* **74**, 1168 (1968).

¹⁵ M. A. Ruderman and C. Kittel, *Phys. Rev.* **96**, 99 (1954).

¹⁶ N. Bloembergen and T. J. Rowland, *Phys.* **97**, 1679 (1955).

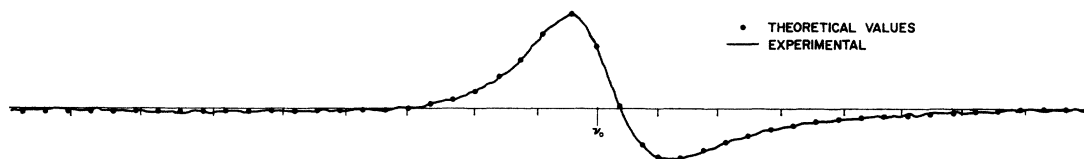


FIG. 1. Isotopically pure Sn¹¹⁹ resonance signal in the [001] direction together with theoretical fit corresponding to the derivative of $\chi'' + b\chi'$, where χ'' is a Lorentzian absorption mode of linewidth 1.45 kHz, χ' is the dispersion mode, and $b=0.68$. The abscissa is marked at intervals of 1 kHz.

It is convenient to rewrite the expression in the form

$$\langle \Delta\omega^2 \rangle = \frac{3}{4}I(I+1)\hbar^2\gamma^4 f \sum (B_{ij}')^2 \times (3 \cos^2\theta_{ij} - 1)^2 r_{ij}^{-6}, \quad (3)$$

where $B_{ij}' = B_{ij}r_{ij}^3/\gamma^2\hbar^2$ is now the ratio between the pseudodipolar and normal dipolar interactions between the given nuclei. As shown in the Appendix, this expression may be analyzed to show that the most general angular variation of the second moment in isotopically pure tin is described by four independent parameters:

$$\langle \Delta\omega^2 \rangle = (A \cos 4\Phi + B) \sin^4\Theta + C \cos^2\Theta \sin^2\Theta + D(3 \cos^2\Theta - 1)^2, \quad (4)$$

where Θ and Φ specify the orientation of the applied magnetic field with respect to the crystallographic axes.

One of the striking characteristics of the above equations for isotopically pure tin is their independence of the scalar exchange coefficient. This, however, does affect the line shape through its contribution to the fourth and higher moments, and in the particular case of a strong scalar exchange interaction, the model of Anderson and Weiss¹⁷ predicts an "exchange-narrowed" Lorentzian line shape having a cutoff of the order of the exchange frequency away from the resonance frequency and resulting in a second moment which is proportional to the linewidth ($\delta\omega$) (defined as the peak separation of the derivative)

$$\langle \Delta\omega^2 \rangle = (\sqrt{3}/\pi)J(\delta\omega), \quad (5)$$

where J is a suitably averaged scalar exchange constant.

EXPERIMENTAL DETAILS

The measurements were made with a Pound-Knight spectrometer upon the isotopically pure Sn¹¹⁹ single crystal described by Schone and Olson.¹⁸ It consisted of a thin-walled hollow cylindrical crystal surrounding a solid copper cylindrical core, and was mounted within the coil of the spectrometer, and oriented with respect to the magnetic field with the aid of x-ray photographs. The measurements were carried out in a 10-kG magnetic field produced by a high homogeneity Varian electromagnet and performed at a temperature of 1.2°K to obtain the largest signals. The natural tin

single crystal was in the form of a cylinder $\frac{3}{8}$ in. diam and 1 in. length of stated purity 99.999% prepared by Metals Research Ltd., Cambridge.

ISOTOPICALLY PURE TIN RESULTS

A typical signal observed with phase-sensitive detection using a 1-sec time constant and magnetic field modulation of amplitude one tenth of the linewidth is shown in Fig. 1. As a consequence of the phase shifts occurring during the penetration of the rf field into the metal, the signal is a mixture of absorption and dispersion mode derivatives.¹⁹

The signal is indistinguishable from a Lorentzian derivative as far out as it is observable, in agreement with free induction decay studies on the same sample¹⁰ and implies that a determination of the second moment from the results is not meaningful. A comparison with the line shapes observed for Sn¹¹⁹ in a sample of natural isotopic abundance suggests that exchange narrowing is responsible for the Lorentzian lines. We would therefore expect the linewidth to show the angular variation predicted for the second moment:

$$(\delta\omega) = (\pi/\sqrt{3}J)\langle \Delta\omega^2 \rangle = (A' \cos 4\Phi + B') \sin^4\Theta + C' \sin^2\Theta \cos^2\Theta + D'(3 \cos^2\Theta - 1)^2. \quad (6)$$

Figures 2 and 3 show the angular variation of the observed linewidth in two orthogonal crystal planes

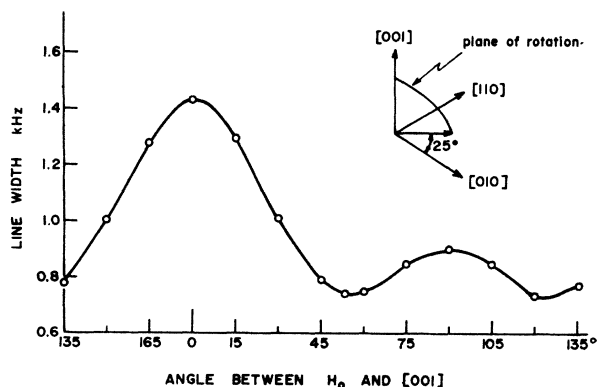


FIG. 2. Angular variation of the linewidth in a plane containing the [001] axis. The solid curve is the fitted theoretical variation.

¹⁷ P. W. Anderson and P. R. Weiss, Rev. Mod. Phys. **25**, 269 (1953).

¹⁸ H. E. Schone and P. W. Olson, Rev. Sci. Instr. **36**, 843 (1965).

¹⁹ A. C. Chapman, P. Rhodes, and E. F. W. Seymour, Proc. Phys. Soc. (London) **B70**, 345 (1957); P. S. Allen and E. F. W. Seymour, *ibid.* **82**, 174 (1963).

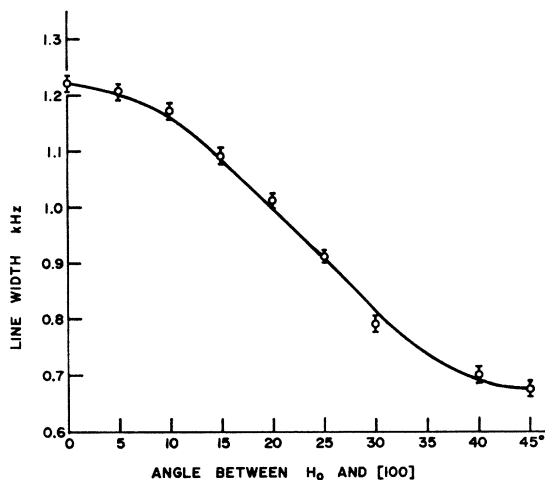


FIG. 3. Angular variation of the linewidth in the basal plane. The solid curve is the fitted theoretical variation.

together with the solid curve resulting from a computer fit to the best values for the four parameters which are $A'=0.28$ kHz, $B'=0.60$ kHz, $C'=2.33$ kHz, and $D'=0.36$ kHz. It should be noted that it is not possible to fit the square of the linewidth to the allowed form, and it is concluded that the results justify the assumption that the linewidth is proportional to the second moment. Indeed this is taken as evidence of exchange narrowing.

However, to determine the coefficients in Eq. (4) it is necessary to relate the linewidth to the second moment in at least one orientation. A number of efforts were made in several orientations by increasing the modulation amplitude to improve the signal-to-noise ratio and thereby to allow the signal to be observed for a further distance from the center frequency. A digital voltmeter was used to monitor the output of the phase-sensitive detector since the signal could not usefully be contained on the chart recorder.

However, despite the fact that the signal under these conditions was sufficiently strong to be observed without phase-sensitive detection on the oscilloscope, we were unable to detect any departure from a Lorentzian shape within the limits of our experimental uncertainty. The final limit here was the determination of the exact position of the baseline and the observation of very

TABLE I. Contributions of various terms to the second moment in natural tin assuming $J=10$ or 12 kHz. The powder linewidth has been inferred from the orientation dependence in the single crystal.

Orientation	Line-width (kHz)	Second moment (kHz) ²	Dipolar and pseudodipolar (kHz) ²		Exchange (kHz) ²	
			10	12	10	12
10° from [001]	1.35	3.9 ± 0.4	0.90	1.08	3.0	2.8
[100]	1.23	3.7 ± 0.4	0.82	0.98	2.9	2.7
Powder	0.92	2.5 ± 0.3	0.61	0.73	1.9	1.8

TABLE II. Relative contributions of neighboring shells of nuclei to the coefficients A , B , C , and D assuming only a direct dipolar interaction.

Shell number	Number of atoms	A	B	C	D
1	4	0.802	0.802	0.955	0.129
2	2	0	0	0	0.302
3	4	0.088	0.088	0.948	0.002
4	8	-0.143	0.143	0.342	0.016
5	4	0.006	0.006	0.178	0.010
6	4	0.018	0.018	0	0.004
7	4	0.001	0.001	0.031	0.005
8	8	-0.004	0.004	0.088	0.003
Sum after 21	120	0.769	1.109	2.684	0.484

weak satellite lines indicating the presence of small misoriented portions of the specimen. On the basis of our observations we concluded that the signal is probably Lorentzian to at least 10 kHz from the center frequency, and thus we have $J \geq 10$ kHz.

NATURAL TIN RESULTS

In an attempt to determine further the exchange parameters, we have also studied the second moment of the resonance line in a tin single crystal of natural isotopic abundance. In this case the second moment is given by the expression (1), which (since $\gamma_1 \approx \gamma_2$) may be rewritten in the form

$$\langle \Delta\omega^2 \rangle = [f_1 + (4/9)f_2] \langle \Delta\omega^2 \rangle_{\text{ISO}} + \frac{1}{3}I(I+1)f_2 \sum J_{ij}^2 - \frac{2}{3}I(I+1)\hbar^{-1}f_2 \sum J_{ij}(B_{ij} + \hbar^2\gamma^2 r_{ij}^{-3}) \times (3 \cos^2\theta_{ij} - 1), \quad (7)$$

where $\langle \Delta\omega^2 \rangle_{\text{ISO}}$ is the second moment for isotopically pure tin given by Eqs. (3) and (5). We may also note that the term in $(3 \cos^2\theta - 1)$ is expected to be small for symmetry reasons and is identically zero when a polycrystalline average is taken. Further, we assume the value of J in the previous equations is equal to $(\sum_i J_{ij})^{1/2}$. This is presumably correct in the weak correlation limit.

Unfortunately, the rather weak signals obtained for natural tin make an accurate determination of the second moment difficult. We have included the two results which we feel are the most reliable together with the value for a powdered specimen determined by Alloul and Deltour.²⁰ In addition, these authors have made spin-echo studies in tin alloys which have led them to suggest that the scalar exchange interaction between nearest neighbors $J_1 = 4.1$ kHz. It is interesting to note that if we assume this value for the six nearest neighbors we obtain $J = 10$ kHz and the term in $\sum_i J_{ij}^2$ yields a contribution to the natural tin second moment of 1.9 (kHz)². In Table I are shown the experimental results for natural tin together with the contributions from the dipolar terms for $J=10$ and 12 kHz. The

²⁰ H. Alloul and R. Deltour, Phys. Rev. **183**, 414 (1969).

difference may be ascribed to the term in $\sum_j J_{ij}^2$ which is predicted to be 1.9 and 2.8 (kHz)², respectively. It should be noted that the neglect of the cross term in $(3 \cos^2\theta - 1)$ is justified experimentally by the similarity between the values for the [001] and [100] orientations, since it can be shown to contribute with opposite sign in the two cases. We therefore conclude from the present results that $J = 11 \pm 1$ kHz and $\sum_j J_{ij}^2 = 120 \pm 20$ (kHz)².

INTERPRETATION

The coefficients A , B , C , and D may now be determined by use of the value $J = 11$ kHz to obtain the values 1.69, 3.64, 14.12, and 2.18 (kHz)², respectively. Whereas the absolute accuracy of these coefficients depends upon the accuracy of J , we note that their relative magnitude is independent of J . We now attempt to relate these to the pseudodipolar coefficients coupling various pairs of nuclei. In particular, it is relevant to note that Eq. (3) contains a dependence upon r_{ij}^{-6} , so that the summation is expected to converge rather rapidly. To illustrate, we show in Table II the contributions from the various shells of neighbors to the constants A , B , C , and D from the dipolar interaction alone (all $B_{ij} = 0$), from which we may observe that the sum over the first four shells is close to the final summation, except in the case of the coefficient C where a 17% contribution still remains. Since we have only four parameters at our disposal, we have considered two special cases: (a) $B_{ij} \neq 0$ for the first four shells of neighbors only; and (b) B_{ij} is constant for all shells outside the third shell, which is consistent with the theoretical form of the interaction at large distances. Table III shows the results for $(1+B_{ij})^2$ obtained in the two cases.

As expected, the third coefficient is the most sensitive to the choice made, since it is clear from Table II that this coefficient makes a dominant contribution to coefficient C . However, the very small difference between the two cases is an encouraging indication of the rapid convergence of the solution and its comparative independence on contributions from neighbors corresponding to $i > 4$. Finally, we have evaluated the two possible values of \bar{B}_{ij} from the results (Fig. 4) together with the expected radial form predicted for a spherical Fermi surface. The deviation is hardly surprising since it is well known that the white-tin Fermi surface deviates considerably from the free-electron sphere.²¹ We note that the contributions to the pseudodipolar interaction from the first four sets of neighbors represent contributions in four different directions, the [201], [001], [023], and [111] directions, respectively. Since the interaction depends upon the Fermi wave vector k_F , the curvature of the Fermi surface, and the nature of the electronic wave functions at extremal points of the Fermi surface, a detailed calculation is necessary to relate the different directions. Such a calculation has

²¹ J. E. Craven and R. W. Stark, Phys. Rev. **168**, 849 (1968).

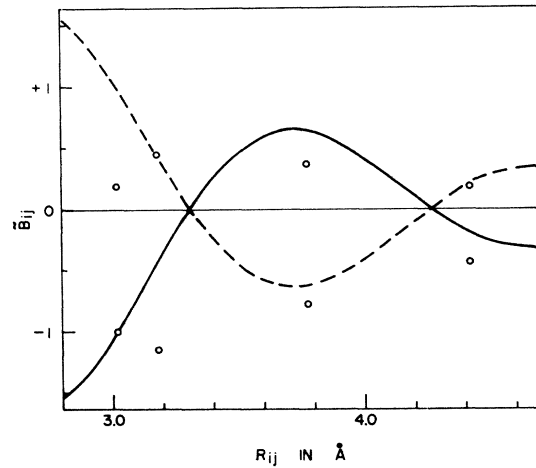


FIG. 4. Possible values of \bar{B}_{ij} compared with the free-electron radial dependence for $k_F = 1.647 \times 10^8$. The theoretical curve (solid line) has been normalized to the value at the first neighbor. The dashed curve is the negative of the solid curve corresponding to the other possible sign of the interaction, and the circles are the experimental points.

recently been performed for lead,²² cesium,²³ and potassium,²³ and in view of the present detailed knowledge of white tin, could readily be carried out here also. A cursory glance at the white-tin Fermi surface in the fourth zone²¹ reveals a hole surface with fairly flat faces perpendicular to the [001] direction, which should give rise to a strong interaction in the direction of the second-nearest neighbors. The actual magnitude will, of course, depend upon the electron wave functions on this piece of surface. In this connection we mention that while the radial dependence of B and J in a given direction is the same, the relative magnitudes of these two quantities may vary according to the electron wave functions which characterize the important pieces of Fermi surface for each direction. We cannot therefore infer the relative magnitudes of J_{ik} for the four shells of neighbors although we may anticipate from the previous Fermi-surface considerations that the coupling between second-nearest neighbors may well be dominant, and it is likely that the coupling of 4.1 kHz measured by Alloul and Deltour is attributable to these.

TABLE III. Values of $(1+B_{ij})^2$ deduced from the experimental results assuming two forms for the contributions from distant neighbors.

	$(1+B_1)^2$	$(1+B_2)^2$	$(1+B_3)^2$	$(1+B_4)^2$
$B_i = B_4$	2.09	5.27	7.53	5.65
$i \geq 4$				
$B_i = 0$	2.08	5.23	7.38	5.58
$i > 4$				

²² L. Tterlikkis, S. D. Mahanti, and T. P. Das, Phys. Rev. Letters **21**, 1796 (1968).

²³ S. D. Mahanti and T. P. Das, Phys. Rev. **170**, 426 (1968).

CONCLUSION

The present work illustrates the detailed information obtainable from single-crystal studies of nuclear-magnetic-resonance lines in metals. (*Note added in proof.* A study of the pseudodipolar interaction for Nb has recently been published by one of the authors.²⁴) Since the results are consistent with an interaction having dipolar symmetry, the work is also an indirect test of the validity of the pseudodipolar approximation. Clearly, a more accurate determination of the natural tin second moments is necessary, or possibly measurements upon some other isotopic composition with a more favorable signal strength. However, the present results are sufficiently accurate to merit a detailed calculation and should prove to be a good test of the electron wave functions in tin.

ACKNOWLEDGMENTS

One of us (S. N. S.) is grateful to the Deans Committee for Research for support. We would like to thank Professor M. Bloom for useful discussions, and we are grateful to Professor E. R. Andrew for drawing our attention to the work of O'Reilly and Tsang. We are also indebted to Dr. H. Alloul and Dr. R. Deltour for a preprint of their work.

APPENDIX

Equation (3) may be rewritten in the form

$$\langle \Delta\omega^2 \rangle = K \sum_j \alpha_{ij} [P_2(\cos\theta_{ij})]^2, \quad (\text{A1})$$

where $K = 3\hbar^2\gamma^4 I(I+1)$, $\alpha_{ij} = (1+B_{ij}')^2 r_{ij}^{-6} P_2(\cos\theta_{ij})$ may be expanded in terms of spherical harmonics according to the equation

$$P_2(\cos\theta_{ij}) = \frac{4}{5}\pi \sum_{m=-2}^{m=+2} Y_{2m}(\theta_{ij}^c, \phi_{ij}^c) Y_{2m}(\Theta, \Phi), \quad (\text{A2})$$

where θ^c , and ϕ^c represent the angles relating r_{ij} to the crystallographic axes and Θ and Φ represent the angles relating the direction of the applied magnetic field to the crystallographic axes.

²⁴ H. E. Schone, Phys. Rev. **183**, 410 (1969).

Substituting (9) into (8) gives

$$\begin{aligned} \langle \Delta\omega^2 \rangle = & K \left(\frac{4}{5}\pi\right)^2 \sum_j \alpha_{ij} \sum_{m=-2}^{m=+2} \sum_{m'=-2}^{m'=+2} Y_{2m}(\theta_{ij}^c, \phi_{ij}^c) \\ & \times Y_{2m'}(\theta_{ij}^c, \phi_{ij}^c) Y_{2m}^*(\Theta, \Phi) Y_{2m'}^*(\Theta, \Phi). \quad (\text{A3}) \end{aligned}$$

This general expression may now be reduced according to the symmetry of the crystal structure. For example, if the crystal has reflection symmetry in the XZ and YZ planes, then in general for a given α_{ij} there will be four atoms with the angular coordinates, $(\theta_{ij}^c, \phi_{ij}^c)$, $(\theta_{ij}^c, -\phi_{ij}^c)$, $(\theta_{ij}^c, \pi - \phi_{ij}^c)$, and $(\theta_{ij}^c, \pi + \phi_{ij}^c)$. The sum over j then involves the following term in ϕ_{ij}^c for arbitrary m and m' :

$$f_{mm'} = e^{i(m+m')\phi_{ij}^c} + e^{-i(m+m')\phi_{ij}^c} + e^{i(m+m')\pi} \times [e^{i(m+m')\phi_{ij}^c} + e^{-i(m+m')\phi_{ij}^c}],$$

which is zero if $(m+m')$ is odd.

Evaluating Eq. (10), retaining only terms with $(m+m')$ even, gives

$$\begin{aligned} \langle \Delta\omega^2 \rangle = & (A'' \cos 4\Phi + B'') [P_{22}(\Theta)]^2 + C'' [P_{21}(\Theta)]^2 \\ & + D'' [P_{20}(\Theta)]^2 + E'' [P_{20}(\Theta)] [P_{22}(\Theta)] \cos 2\Phi \\ & + F'' [P_{21}(\Theta)]^2 \cos 2\Phi, \quad (\text{A4}) \end{aligned}$$

where

$$A'' = \sum_j \alpha_{ij} A_{ij}'',$$

and

$$A_{ij}'' = \left(\frac{4}{5}\pi\right)^2 2K [P_{22}(\theta_{ij}^c)]^2 \cos(4\phi_{ij}^c),$$

$$B'' = \sum_j \alpha_{ij} B_{ij}'',$$

and

$$B_{ij}'' = \left(\frac{4}{5}\pi\right)^2 2K [P_{22}(\theta_{ij}^c)]^2, \text{ etc.}$$

For tetragonal symmetry, the equation is further reduced since no term in $\cos(2\Phi)$ is allowed, and we obtain Eq. (4).

Subsequent to deriving this result, the work of O'Reilly and Tsang²⁵ was brought to our attention, which confirms the fact that four independent parameters are required to specify the most general allowed angular variation of the second moment in the tin crystal structure.

²⁵ D. E. O'Reilly and Tung Tsang, Phys. Rev. **128**, 2639 (1962).